Linear Phase Paraunitary Filter Bank with Filters of Different Lengths and its Application in Image Compression

Trac D. Tran, *Member, IEEE*, Maasaki Ikehara, *Member, IEEE*, and Truong Q. Nguyen, *Senior Member, IEEE*

***Abstract*— In this paper, the theory, structure, design, and implementation of a new class of linear-phase paraunitary filter banks (LPPUFB's) are investigated. The novel filter banks with filters of different lengths can be viewed as the generalized lapped orthogonal transforms (GenLOT's) with variable-length basis functions. Our main motivation is the application in block-transform-based image coding. Besides having all of the attractive properties of other lapped orthogonal transforms, the new transform takes advantage of its long, overlapping basis functions to represent smooth signals in order to reduce blocking artifacts, whereas it reserves short basis functions for high-frequency signal components like edges and texture, thereby limiting ringing artifacts. Two design methods are presented, each with its own set of advantages: The first is based on a direct lattice factorization, and the second enforces certain relationships between the lattice coefficients to obtain variable length filters. Various necessary conditions for the existence of meaningful solutions are derived and discussed in both cases. Finally, several design and image coding examples are presented to confirm the validity of the theory.**

***Index Terms*— Filter bank, image compression, linear-phase filter bank, linear-phase paraunitary filter bank.**

I. Introduction

FROM A FILTER bank perspective, the lapped orthogonal transform (LOT) and its generalized version GenLOT belong to a subclass of maximally decimated M-channel FIR real-coefficient linear phase perfect reconstruction filter banks (see Fig. 1) [1], [2]. From the polyphase representation in Fig. 1(b) and ignoring any processing of the coefficients, perfect reconstruction can be achieved by designing $\mathbf{E}(z)$ appropriately such that $\mathbf{R}(z)$ can be chosen as

$$\mathbf{R}(z) = z^{-K}\mathbf{E}^T\left(z^{-1}\right) \tag{1}$$

where K is the order of $\mathbf{E}(z)$. Such a system is called *paraunitary*. Soman *et al.* first introduced a complete and minimal factorization [3] that covers a large class of linear phase paraunitary filter banks (LPPUFB's): even-channel M with all of the filters having the same length MK. The complete factorization assures that all possible solutions in the assumed class are covered by the structure, whereas minimality provides the most efficient implementation in term of the number of delay elements needed.

An equivalent, but modular, factorization called GenLOT is presented in [4], where the authors showed that the DCT and the LOT are low-order special cases. The GenLOT is simply the aforementioned class of LPPUFB implemented as a block transform. It provides an elegant solution to the elimination of blocking artifacts in traditional block-transform image coders. A direct implementation of the GenLOT is depicted in Fig. 2. The input signal can be blocked into sequences of length $L = MK$, with adjacent sequences being overlapped by $M(K-1)$ samples. The M columns of the transposed transform coefficient matrix $\mathbf{P}$ hold the impulse responses of the analysis filters $h_i[n]$. The resulting M subband signals $y_i[n]$ can then be quantized, coded, and transmitted to the decoder, where the inverse transform is performed to reconstruct the signal. Due to the transpositional relationship between $\mathbf{E}(z)$ and $\mathbf{R}(z)$, the inverse transform matrix turns out to be $\mathbf{P}$, whose rows store the synthesis filters' impulse responses. The GenLOT's orthogonality provides good energy compaction and leads to elegant bit allocation algorithms. Its long basis functions that decay smoothly to zero, coupled with overlapping data blocks, reduce blocking artifacts at high compression ratios.

The GenLOT possesses an efficient lattice structure that retains both linear phase and paraunitary properties under the quantization of lattice coefficients. However, the lattice structure of GenLOT imposes a very strict restriction on both analysis and synthesis filters. They must have the same length, which is a multiple of the number of channels. In this paper, we present a family of lapped transforms called VLLOT, which are designed with a different philosophy: The basis functions can have different lengths.

There are numerous motivations for studying transforms with basis functions of variable length. First of all, it is quite natural to represent slowly changing signals by long basis functions. On the other hand, fast-changing, high-frequency components such as edges and textures in images are better captured by short basis functions. The wavelet transform

Manuscript received December 12, 1997; revised February 25, 1998. This work was supported in part by the National Science Foundation under Grant MIP-9501589. The associate editor coordinating the review of this paper and approving it for publication was Dr. Frans M. Coetzee.

T. D. Tran was with the Department of Electrical and Computer Engineering, University of Wisconsin, Madison, WI 53706 USA. He is now with the Department of Electrical and Computer Engineering, The Johns Hopkins University, Baltimore, MD 21218 USA (e-mail: ttran@ece.jhu.edu).

M. Ikehara is with the Department of Science and Technology, Keio University, Yokohama, Japan (e-mail: ikehara@saigon.ece.wisc.edu).

T. Q. Nguyen is with the Department of Electrical and Computer Engineering, Boston University, Boston, MA 02215 USA (e-mail: nguyent@bu.edu).

Publisher Item Identifier S 1053-587X(99)07569-8.

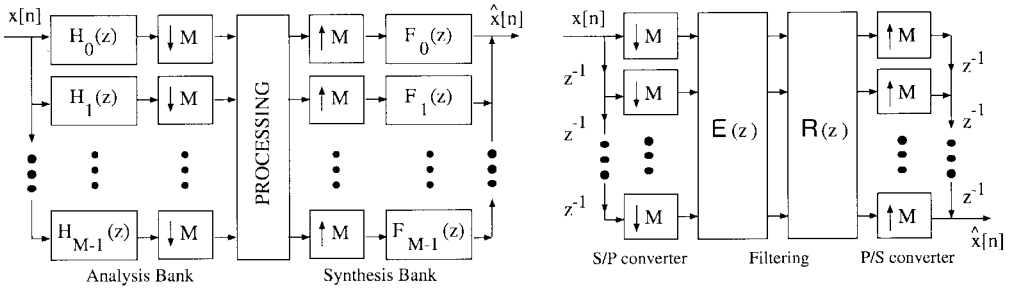

Fig. 1. Two representations of an M-channel uniform-band maximally-decimated filter bank.

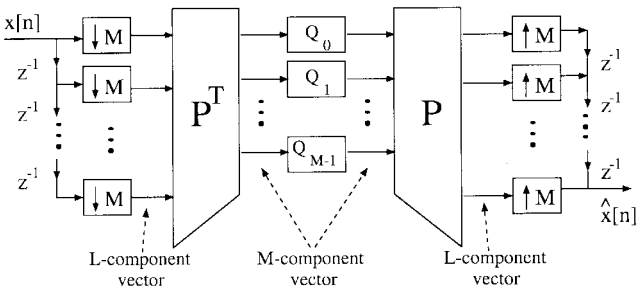

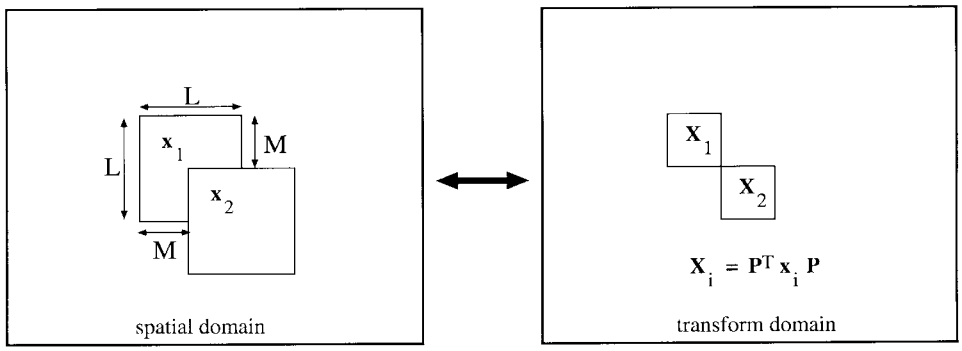

Fig. 2. M-channel LPPUFB as lapped transform. (a) Direct implementation in 1-D. (b) Illustration in 2-D.

serves as a wonderful illustration of this intuitive concept. From the lapped transform perspective, it is advantageous for the transform to have a set of varying-length basis. Long basis functions mean larger overlap of input data and smoother impulse responses, leading to a reduction of blocking artifacts in the reconstructed images. Unfortunately, long basis functions are also the main contributors to severe ringing around strong edges, where huge quantization errors are spread out to smoother neighborhood regions. Hence, longer basis functions should only be reserved for low-frequency components, whereas shorter basis functions should be employed to represent high-frequency components.

Most importantly, the longer the filter becomes, the higher the complexity of the FB gets. Since blocking is most noticeable in smooth image regions, in order to reduce blocking artifacts, filters covering high-frequency bands do not need long overlapping windows. In fact, they may not have to be overlapped at all. If the filter length can be restricted mathematically, i.e., these coefficients are structurally enforced to exact zeros, the complexity of the resulting FB can be reduced significantly.

A. Outline

The outline of the paper is as follows. In Section II, we offer a brief review of GenLOT's lattice structure and its design procedure. Section III derives a complete and minimal lattice structure for VLLOT. Section IV describes a different design approach based on the relationship between GenLOT's building blocks. In both methods, various necessary conditions for the existence of meaningful solutions are discussed. Section V presents the VLLOT design procedure based on unconstrained nonlinear optimization and several design examples. Next, image coding examples illustrating the advantages of the new transforms are presented in Section VI. Finally, Section VII draws up the final conclusions.

B. Notation

Notation-wise, bold-faced characters are reserved to denote vectors and matrices. $\mathbf{A}^T$, $|\mathbf{A}|$, $\mathbf{a}_{i,}$, $\mathbf{a}_{,j}$ stand for the transpose, the determinant, the ith row, and the jth column of the matrix $\mathbf{A}$. Special matrices used extensively are the identity matrix $\mathbf{I}$, the reversal matrix $\mathbf{J}$, and the null matrix $\mathbf{0}$. When the

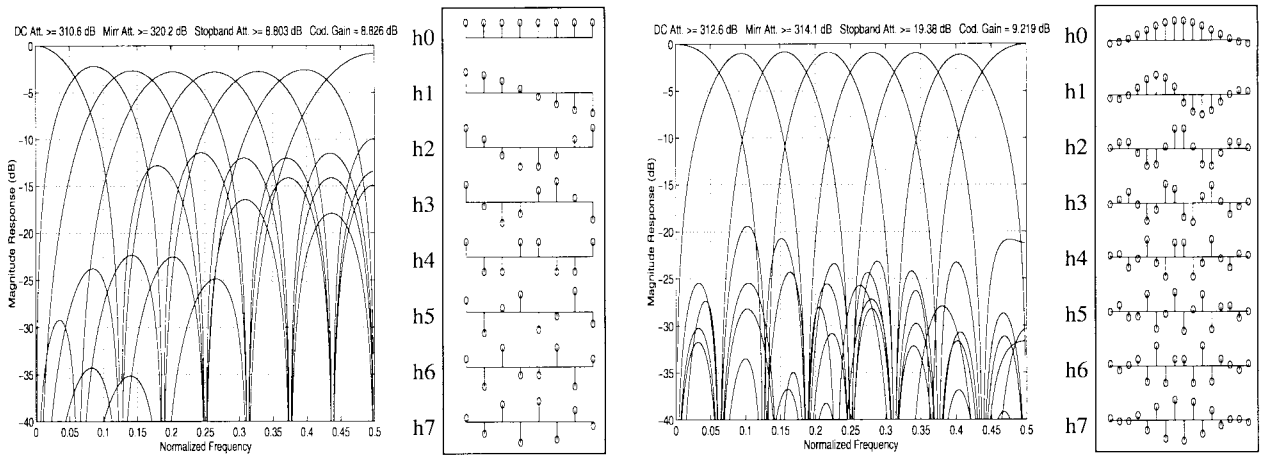

(a) (b)

Fig. 3. Frequency and impulse responses of popular block transforms. (a) DCT, eight channels, all eight-tap filters. (b) LOT, eight channels, all 16-tap filters.

size of a matrix is not clear from context, subscripts will be included to indicate its size. For example, $\mathbf{J}_M$ denotes the square $M \times M$ reversal matrix, whereas $\mathbf{0}_{M\times N}$ stands for the $M \times N$ null matrix. $\mathcal{S}\{\mathbf{a}_1, \mathbf{a}_2, \cdots, \mathbf{a}_n\}$ is used to represent the vector space spanned by the n vectors $\mathbf{a}_1, \mathbf{a}_2, \cdots, \mathbf{a}_n$. For abbreviations, we use LP, PR, PU, VL, and FB to denote, respectively, *linear phase, perfect reconstruction, paraunitary, variable length,* and *filter bank*. The letters M and L are reserved for the number of channels and the filter's length. The terms LPPUFB and GenLOT, LPPUFB with filters of different lengths and VLLOT, are used interchangeably in the paper.

II. Review

LPPUFB's have long found application in transform-based image coding. For example, the discrete cosine transform (DCT) as shown in Fig. 3(a) is an M-channel M-tap LPPUFB that has been widely used in the international image compression standard JPEG [5]. A popular extension of the DCT is the lapped orthogonal transform (LOT), which is an even-channel $2M$-tap LPPUFB [see Fig. 3(b)] that can be interpreted as an overlapping block transform [6]. To reduce the blocking effect further, longer data overlaps are needed. This motivates the development of the GenLOT [4]. The most general lapped transform lattice structure up to date is presented in [7], where the authors are able to parameterize the complete class of all even-channel LPPUFB's.

An attractive approach to the design and implementation of LPPUFB is the FB's parameterization by a lattice structure. The lattice structure offers fast, efficient implementation and retains both LP and PU properties, regardless of coefficient quantization. The key idea in obtaining a lattice structure is the factorization of the FB's polyphase matrix $\mathbf{E}(z)$. Let $H_k(z)$ and $F_k(z)$ be the analysis and synthesis filters of length $L = MK$ in an M-channel LPPUFB. If M is even, it is necessary to have $M/2$ symmetric and $M/2$ antisymmetric filters [7]. Define

$$\mathbf{\Phi}_i = \begin{bmatrix} \mathbf{U}_i & \mathbf{0}_{M/2} \\ \mathbf{0}_{M/2} & \mathbf{V}_i \end{bmatrix} \tag{2}$$

where $\mathbf{U}_i$ and $\mathbf{V}_i$ are arbitrary $M/2 \times M/2$ orthogonal matrices, and let

$$\mathbf{W} = \frac{1}{\sqrt{2}} \begin{bmatrix} \mathbf{I}_{M/2} & \mathbf{I}_{M/2} \\ \mathbf{I}_{M/2} & -\mathbf{I}_{M/2} \end{bmatrix}$$
$$\mathbf{\Lambda} = \begin{bmatrix} \mathbf{I}_{M/2} & \mathbf{0}_{M/2} \\ \mathbf{0}_{M/2} & z^{-1}\mathbf{I}_{M/2} \end{bmatrix}. \tag{3}$$

Then, the polyphase matrix $\mathbf{E}(z)$ can always be factored as [4]

$$\mathbf{E}(z) = \mathbf{G}_{K-1}(z)\mathbf{G}_{K-2}(z) \cdots \mathbf{G}_1(z)\mathbf{E}_0 \tag{4}$$

where $\mathbf{G}_i(z) = \mathbf{\Phi}_i\mathbf{W}\mathbf{\Lambda}(z)\mathbf{W}$, and

$$\mathbf{E}_0 = \begin{bmatrix} \mathbf{U}_0 & \mathbf{U}_0\mathbf{J}_{M/2} \\ \mathbf{V}_0\mathbf{J}_{M/2} & -\mathbf{V}_0 \end{bmatrix}$$
$$= \begin{bmatrix} \mathbf{U}_0 & \mathbf{0}_{M/2} \\ \mathbf{0}_{M/2} & \mathbf{V}_0 \end{bmatrix} \begin{bmatrix} \mathbf{I}_{M/2} & \mathbf{J}_{M/2} \\ \mathbf{J}_{M/2} & -\mathbf{I}_{M/2} \end{bmatrix}. \tag{5}$$

Again, $\mathbf{U}_0$ and $\mathbf{V}_0$ are arbitrary $M/2 \times M/2$ orthogonal matrices. For fast implementation, $\mathbf{E}_0$ can be replaced by the DCT [4], [6]. It is clear from (2)–(5) that each stage of GenLOT [either $\mathbf{G}_i(z)$ or $\mathbf{E}_0$] contains two arbitrary orthogonal matrices of size $M/2$. Therefore, the most general GenLOT of order $(K-1)$ can be parametrized by $2K\binom{M/2}{2}$ rotation angles and requires $(M(K-1))/2$ delays in its implementation. The complete and minimal lattice structure is shown in Fig. 4.

More generally, Tran *et al.* show that a modification to the initial stage produces GenLOT with filters of length $L = MK + \beta$, i.e., $\mathbf{E}_0$ will no longer be a simple zero-order matrix [7]. The authors also present several interesting necessary existence conditions on the FB's symmetry polarity and lengths, which can be summarized in Table I [7]. From this table of permissible solutions, it is a simple exercise to show that odd-length GenLOT does not exist.

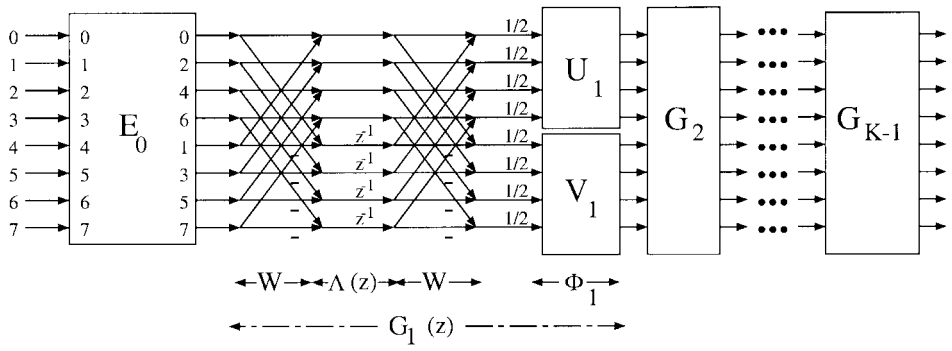

Fig. 4. General lattice structure for LPPUFB's.

TABLE I
POSSIBLE SOLUTIONS FOR M-CHANNEL LPPRFB WITH FILTER LENGTHS $L_i = MK_i + \beta$

Case	*Symmetry Polarity Condition*	*Length Condition*	*Sum of Lengths*
M even, β even	$\frac{M}{2}$ S & $\frac{M}{2}$ A	$\sum K_i$ even	$2mM$
M even, β odd	$(\frac{M}{2}+1)$ S & $(\frac{M}{2}-1)$ A	$\sum K_i$ odd	$2mM$
M odd, β even	$(\frac{M+1}{2})$ S & $(\frac{M-1}{2})$ A	$\sum K_i$ odd	$(2m+1)M$
M odd, β odd	$(\frac{M+1}{2})$ S & $(\frac{M-1}{2})$ A	$\sum K_i$ even	$(2m+1)M$

III. VLLOT LATTICE STRUCTURE

A. Problem Formulation

This section presents a lattice structure for LPPUFB with filters of different lengths. For purposes of simplicity, we shall first consider systems with filters of lengths $L_i = MK_i$, where M is even, and

$$K_i = \begin{cases} K, & \text{for } 0 \le i \le N-1 \le M-1 \\ K-1, & \text{for } N \le i \le M-1. \end{cases}$$

Simply speaking, the class of LPPUFB under investigation has N long filters of length MK and $(M-N)$ shorter filters of length $M(K-1)$.

B. Existence Conditions

Theorem I: For the class of even-channel LPPUFB's described above, the number of long filters and the number of short filters must both be even.

Proof: The FB has a total length of

$$\begin{aligned} \sum_{i=0}^{M-1} L_i &= NMK + (M-N)M(K-1) \\ &= M(NK + MK - NK - M + N) \\ &= M(MK - M + N). \end{aligned}$$

From Table I, for even M, $(MK - M + N)$ has to be even. Since M is even, $MK - M$ is even for any K. Therefore, N has to be even, and so is $(M-N)$, i.e., there are an even number of long, as well as short, filters. □

Theorem II: In a LPPUFB with N filters of length MK and $(M-N)$ filters of length $M(K-1)$, half of the long filters are symmetric, and half of the short filters are symmetric.

Proof: Let $\mathbf{L}(z)$ be the $N \times M$ polyphase matrix of order $(K-1)$, representing the longer filters, and let $\mathbf{S}(z)$ be the $(M-N)\times M$ polyphase matrix of order $(K-2)$, representing the shorter filters. Without any loss of generality, the long filters are permuted to be on top. Since $\mathbf{E}(z)$ is paraunitary, we have

$$\begin{aligned} \mathbf{E}(z)\mathbf{E}^T(z^{-1}) &= \begin{bmatrix} \mathbf{L}(z) \\ \mathbf{S}(z) \end{bmatrix} \begin{bmatrix} \mathbf{L}^T(z^{-1}) & \mathbf{S}^T(z^{-1}) \end{bmatrix} \\ &= \begin{bmatrix} \mathbf{L}(z)\mathbf{L}^T(z^{-1}) & \mathbf{L}(z)\mathbf{S}^T(z^{-1}) \\ \mathbf{S}(z)\mathbf{L}^T(z^{-1}) & \mathbf{S}(z)\mathbf{S}^T(z^{-1}) \end{bmatrix} \\ &= \mathbf{I}_M \end{aligned} \tag{6}$$

and

$$\begin{aligned} \mathbf{E}^T(z^{-1})\mathbf{E}(z) &= \begin{bmatrix} \mathbf{L}^T(z^{-1}) & \mathbf{S}^T(z^{-1}) \end{bmatrix} \begin{bmatrix} \mathbf{L}(z) \\ \mathbf{S}(z) \end{bmatrix} \\ &= \mathbf{L}^T(z^{-1})\mathbf{L}(z) + \mathbf{S}^T(z^{-1})\mathbf{S}(z) \\ &= \mathbf{I}_M. \end{aligned} \tag{7}$$

Furthermore, $\mathbf{E}(z)$ also has to satisfy the LP property in [3] and [7]

$$\begin{aligned} \mathbf{E}(z) &= \begin{bmatrix} \mathbf{L}(z) \\ \mathbf{S}(z) \end{bmatrix} \\ &= \begin{bmatrix} z^{-(K-1)}\mathbf{I}_N & \mathbf{0} \\ \mathbf{0} & z^{-(K-2)}\mathbf{I}_{M-N} \end{bmatrix} \begin{bmatrix} \mathbf{D}_L & \mathbf{0} \\ \mathbf{0} & \mathbf{D}_S \end{bmatrix} \\ &\quad \cdot \begin{bmatrix} \mathbf{L}(z^{-1}) \\ \mathbf{S}(z^{-1}) \end{bmatrix} \begin{bmatrix} \mathbf{0} & \mathbf{J} \\ \mathbf{J} & \mathbf{0} \end{bmatrix} \end{aligned} \tag{8}$$

where $N \times N$ $\mathbf{D}_L$ and $(M-N) \times (M-N)$ $\mathbf{D}_S$ are diagonal matrices whose entry is $+1$ when the corresponding filter is symmetric and -1 when the corresponding filter is antisymmetric. The traces of these two matrices hold the key to the number of long (as well as short) symmetric and antisymmetric filters.

From (8), we can obtain the following relationships:

$$\begin{cases} \mathbf{L}(z) = z^{-(K-1)}\mathbf{D}_L\mathbf{L}(z^{-1})\mathbf{J}_M \\ \mathbf{S}(z) = z^{-(K-2)}\mathbf{D}_S\mathbf{S}(z^{-1})\mathbf{J}_M. \end{cases} \tag{9}$$

Since $\mathbf{L}(z)\mathbf{L}^T(z^{-1}) = \mathbf{I}_N$ and $\mathbf{S}(z)\mathbf{S}^T(z^{-1}) = \mathbf{I}_{M-N}$ from (6), solving for $\mathbf{D}_L$ and $\mathbf{D}_S$ yields

$$\begin{cases} \mathbf{D}_L = z^{-(K-1)}\mathbf{L}(z^{-1})\mathbf{J}_M\mathbf{L}^T(z^{-1}) \\ \mathbf{D}_S = z^{-(K-2)}\mathbf{S}(z^{-1})\mathbf{J}_M\mathbf{S}^T(z^{-1}). \end{cases} \tag{10}$$

Taking the trace of both sides and using the fact that $\mathrm{tr}(\mathbf{AB}) = \mathrm{tr}(\mathbf{BA})$, we can obtain

$$\begin{cases} \mathrm{tr}(\mathbf{D}_L) = \mathrm{tr}\Big(z^{-(K-1)}\mathbf{L}(z^{-1})\mathbf{J}_M\mathbf{L}^T(z^{-1})\Big) \\ \qquad\quad = \mathrm{tr}\Big(z^{-(K-1)}\mathbf{L}^T(z^{-1})\mathbf{L}(z^{-1})\mathbf{J}_M\Big) \\ \mathrm{tr}(\mathbf{D}_S) = \mathrm{tr}\Big(z^{-(K-2)}\mathbf{S}(z^{-1})\mathbf{J}_M\mathbf{S}^T(z^{-1})\Big) \\ \qquad\quad = \mathrm{tr}\Big(z^{-(K-2)}\mathbf{S}^T(z^{-1})\mathbf{S}(z^{-1})\mathbf{J}_M\Big). \end{cases} \tag{11}$$

$\mathrm{Tr}(\mathbf{D}_L)$ and $\mathrm{tr}(\mathbf{D}_S)$ are constants, and therefore, their values can be obtained by evaluating the right-hand sides of the above equation at any specific value of z. First, let us consider the case of even K. Evaluating (11) at $z = 1$, we have

$$\begin{cases} \mathrm{tr}(\mathbf{D}_L) = \mathrm{tr}\big(\mathbf{L}^T(1)\mathbf{L}(1)\mathbf{J}_M\big) \\ \mathrm{tr}(\mathbf{D}_S) = \mathrm{tr}\big(\mathbf{S}^T(1)\mathbf{S}(1)\mathbf{J}_M\big). \end{cases} \tag{12}$$

Evaluating (11) at $z = -1$ yields

$$\begin{cases} \mathrm{tr}(\mathbf{D}_L) = -\mathrm{tr}\big(\mathbf{L}^T(-1)\mathbf{L}(-1)\mathbf{J}_M\big) \\ \mathrm{tr}(\mathbf{D}_S) = \mathrm{tr}\big(\mathbf{S}^T(-1)\mathbf{S}(-1)\mathbf{J}_M\big). \end{cases} \tag{13}$$

From (7), we also have

$$\begin{cases} \mathbf{L}^T(1)\mathbf{L}(1)\mathbf{J}_M + \mathbf{S}^T(1)\mathbf{S}(1)\mathbf{J}_M = \mathbf{J}_M \\ \mathbf{L}^T(-1)\mathbf{L}(-1)\mathbf{J}_M + \mathbf{S}^T(-1)\mathbf{S}(-1)\mathbf{J}_M = \mathbf{J}_M. \end{cases}$$

Hence, since $\mathrm{tr}(\mathbf{J}_M) = 0$

$$\begin{aligned} \mathrm{tr}(\mathbf{D}_L) &= \mathrm{tr}\big(\mathbf{L}^T(1)\mathbf{L}(1)\mathbf{J}_M\big) \\ &= \mathrm{tr}\big(\mathbf{J}_M - \mathbf{S}^T(1)\mathbf{S}(1)\mathbf{J}_M\big) \\ &= \mathrm{tr}(\mathbf{J}_M) - \mathrm{tr}\big(\mathbf{S}^T(1)\mathbf{S}(1)\mathbf{J}_M\big) \\ &= -\mathrm{tr}\big(\mathbf{S}^T(1)\mathbf{S}(1)\mathbf{J}_M\big). \end{aligned}$$

On the other hand

$$\begin{aligned} \mathrm{tr}(\mathbf{D}_L) &= -\mathrm{tr}\big(\mathbf{L}^T(-1)\mathbf{L}(-1)\mathbf{J}_M\big) \\ &= -\mathrm{tr}\big(\mathbf{J}_M - \mathbf{S}^T(-1)\mathbf{S}(-1)\mathbf{J}_M\big) \\ &= -\mathrm{tr}(\mathbf{J}_M) + \mathrm{tr}\big(\mathbf{S}^T(-1)\mathbf{S}(-1)\mathbf{J}_M\big) \\ &= \mathrm{tr}\big(\mathbf{S}^T(1)\mathbf{S}(1)\mathbf{J}_M\big). \end{aligned}$$

Therefore, $\mathrm{tr}(\mathbf{S}^T(1)\mathbf{S}(1)\mathbf{J}_M) = 0$, leading to the desired result that $\mathrm{tr}(\mathbf{D}_L) = 0$, and $\mathrm{tr}(\mathbf{D}_S) = 0$. In other words, half of the longer filters are symmetric, whereas the remaining half are antisymmetric. Similarly, half of the short filters are symmetric, and the rest are antisymmetric. It is a simple exercise to verify that the same conclusion can be reached for the case of odd K. □

C. Lattice Structure

From Theorem II, there are $N/2$ long symmetric filters and $N/2$ long antisymmetric filters. If the long symmetric filters are permuted to be on top, i.e.,

$$\mathbf{D}_L = \begin{bmatrix} \mathbf{I}_{N/2} \\ -\mathbf{I}_{N/2} \end{bmatrix}$$

they now form a remarkably similar system to an N-channel order-$(K-1)$ GenLOT

$$\mathbf{L}(z) = z^{-(K-1)}\mathbf{D}_L\mathbf{L}(z^{-1})\mathbf{J}_M. \tag{14}$$

From [4], there exists a factorization [shown in (4)] that reduces the order of the polyphase matrix $\mathbf{L}(z)$ by one. Hence, the VLLOT's polyphase matrix $\mathbf{E}(z)$ can always be factored as

$$\begin{aligned} \mathbf{E}(z) &= \hat{\mathbf{G}}_0(z)\mathbf{E}_{K-2}(z) \\ &= \hat{\mathbf{\Phi}}_0\hat{\mathbf{W}}\hat{\mathbf{\Lambda}}(z)\hat{\mathbf{W}}\hat{\mathbf{P}}_0\mathbf{E}_{K-2}(z) \end{aligned} \tag{15}$$

where

$$\begin{aligned} \hat{\mathbf{W}} &= \begin{bmatrix} \mathbf{I_{N/2}} & \mathbf{I_{N/2}} & \mathbf{0} \\ \mathbf{I_{N/2}} & -\mathbf{I_{N/2}} & \mathbf{0} \\ \mathbf{0} & \mathbf{0} & \mathbf{I_{M-N}} \end{bmatrix} \\ \hat{\mathbf{\Lambda}}(z) &= \begin{bmatrix} \mathbf{I_{N/2}} & \mathbf{0} & \mathbf{0} \\ \mathbf{0} & z^{-1}\mathbf{I_{N/2}} & \mathbf{0} \\ \mathbf{0} & \mathbf{0} & \mathbf{I_{M-N}} \end{bmatrix}, \end{aligned} \tag{16}$$

and

$$\hat{\mathbf{\Phi}}_0 = \begin{bmatrix} \hat{\mathbf{U}}_0 & \mathbf{0} & \mathbf{0} \\ \mathbf{0} & \hat{\mathbf{V}}_0 & \mathbf{0} \\ \mathbf{0} & \mathbf{0} & \mathbf{I_{M-N}} \end{bmatrix}. \tag{17}$$

$\hat{\mathbf{P}}_0$ is the permutation matrix that arranges the longer filters on top, i.e.,

$$\hat{\mathbf{P}}_0 = \begin{bmatrix} \mathbf{I_{N/2}} & \mathbf{0} & \mathbf{0} & \mathbf{0} \\ \mathbf{0} & \mathbf{0} & \mathbf{I_{N/2}} & \mathbf{0} \\ \mathbf{0} & \mathbf{I_{(M-N)/2}} & \mathbf{0} & \mathbf{0} \\ \mathbf{0} & \mathbf{0} & \mathbf{0} & \mathbf{I_{(M-N)/2}} \end{bmatrix}.$$

It is added to simplify the presentation only. Note that the above factorization leaves $\mathbf{S}(z)$ untouched; it reduces the length of the longer filters by M so that all filters now have the same length of $M(K-1)$. $\mathbf{E}_{K-2}(z)$ is the familiar polyphase matrix of an order-$(K-2)$ GenLOT. The rotation angles of $N/2 \times N/2$ orthogonal matrices $\hat{\mathbf{U}}_0$ and $\hat{\mathbf{V}}_0$ are the stage's free parameters that can be varied independently and arbitrarily to optimize the VLLOT. Comparing with the traditional order-$(K-1)$ GenLOT, the number of free parameters is reduced by $2\binom{M/2}{2} - 2\binom{N/2}{2}$. The reduction can be quite significant if the number of channels M is large and the number of long filters N is small. For the case that $N = 2$, the number of free parameters comes from $\mathbf{E}_{K-2}(z)$ only: $\hat{\mathbf{U}}_0$ and $\hat{\mathbf{V}}_0$ become singletons ± 1.

As previously mentioned, with $\hat{\mathbf{G}}_0(z)$ peeled off, $\mathbf{E}_{K-2}(z)$ becomes the familiar polyphase matrix of an order-$(K-2)$ GenLOT. Hence, it can be factored by the conventional methods [4]. An example of the detailed lattice is illustrated in Fig. 5.

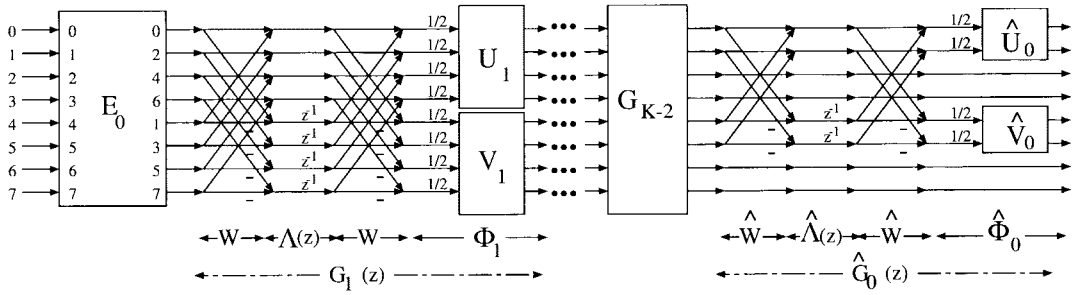

Fig. 5. Detailed lattice structure for the VLLOT (drawn for $M = 8$ and $N = 4$).

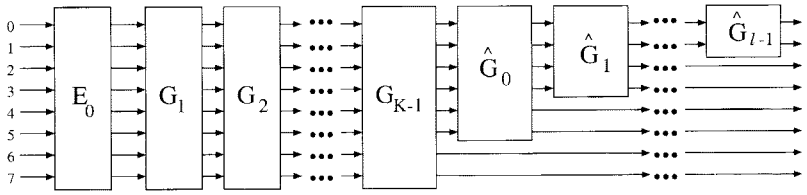

Fig. 6. General lattice structure for the VLLOT.

Theorem III: The proposed factorization of $\mathbf{E}(z)$ in (15) is minimal, i.e., the lattice structure uses the fewest possible number of delays in the implementation.

Proof: A structure is defined to be minimal when the required number of delays is equal to the degree of the transfer function [1]. For paraunitary systems, it has been proven in [1] that $\deg(\mathbf{E}(z)) = \deg(|\mathbf{E}(z)|)$.

Exploiting the LP property of the FB polyphase matrix in (8), we have

$$\begin{aligned}\deg(\mathbf{E}(z)) &= \deg(|\mathbf{E}(z)|)\\ &= \deg\left(\begin{vmatrix} z^{-(K-1)}\mathbf{I}_N & \mathbf{0} \\ \mathbf{0} & z^{-(K-2)}\mathbf{I}_{M-N}\end{vmatrix} \begin{vmatrix}\mathbf{D}_L & \mathbf{0}\\ \mathbf{0} & \mathbf{D}_S\end{vmatrix} \begin{vmatrix}\mathbf{L}(z^{-1}) \\ \mathbf{S}(z^{-1})\end{vmatrix} \begin{vmatrix}\mathbf{0} & \mathbf{J}\\ \mathbf{J} & \mathbf{0}\end{vmatrix}\right)\\ &= N(K-1) + (M-N)(K-2) - \deg(\mathbf{E}(z)).\end{aligned}$$

Hence

$$\begin{aligned}\deg(\mathbf{E}(z)) &= \frac{N(K-1)+(M-N)(K-2)}{2}\\ &= \frac{M(K-2)}{2} + \frac{N}{2}.\end{aligned}$$

In the proposed factorization, we use $(M(K-2))/2$ delays for $\mathbf{E}_{K-2}(z)$ and $N/2$ for $\hat{\mathbf{G}}_0(z)$, totaling the same number of delays as the degree of $\mathbf{E}(z)$. Therefore, the factorization is minimal. □

It is interesting to note that when N increases to M or decreases to 0, the VLLOT's required number of delay elements increases to $(M(K-1))/2$ or decreases to $(M(K-2))/2$, which is consistent with the delays needed in GenLOT's implementation [4].

More general and complicated VLLOT can be constructed by a cascade of building blocks $\hat{\mathbf{G}}_i$ as

$$\begin{aligned}\mathbf{E}(z) = &\hat{\mathbf{G}}_{\ell-1}(z)\cdots\hat{\mathbf{G}}_1(z)\hat{\mathbf{G}}_0(z)\mathbf{G}_{K-1}(z)\cdots\\ &\mathbf{G}_1(z)\mathbf{G}_0(z)\end{aligned} \tag{18}$$

where $N_0 \geq N_1 \geq \cdots \geq N_{\ell-1}$, and each N_i is even. The longest filters have length $M(K+\ell)$, whereas the shortest filters have length MK. The general lattice structure is depicted in Fig. 6.

IV. VLLOT via Orthogonal Complement Subspaces

In the lattice structure design method presented in the previous section, the filters' centers of symmetry are not aligned. The alignment of the bases is sometimes desired since it provides more accurate correlation between subband signals, and it simplifies the signal's symmetric extension [8], [9]. Only in cases in which the length difference between the long and the short filters are even multiples of M, the alignment of the centers of symmetry can be obtained by shifting the short filters (at the cost of adding more delay elements of course).

A. Problem Formulation

In this section, another class of VLLOT whose filters all share the same center of symmetry is studied. These FB's can be thought of as a GenLOT subclass, where the tail-end coefficients of some filters are forced to be zero. More specifically, given an M-channel GenLOT of length MK with M even, we are interested in the relationships between the building blocks $\mathbf{U}_i$, $\mathbf{V}_i$ in (4) such that the resulting $M \times MK$ coefficients matrix $\mathbf{P}_K$ (or a simple row permutation of $\mathbf{P}_K$) satisfies the following variable-length condition as shown in (19) at the bottom of the next page. Simply speaking, we are studying a GenLOT subclass of order $(K-1)$, where all of the filters share the same center of symmetry, N filters have length MK, and the remaining $(M-N)$ filters have length $M(K-1)$.

B. Existence Condition

Theorem IV: It is impossible to construct a VLLOT described in the problem formulation above with all symmetric (or all antisymmetric) filters being shortened by M taps.

Proof: It is a straightforward but tedious exercise to show that the left tail end of the GenLOT coefficient matrix turns out to be as shown in (20) at the bottom of the page [4]. Suppose that all antisymmetric filters are short; then $\mathbf{V}_{K-1}\prod_{i=K-2}^{0}(\mathbf{U}_i-\mathbf{V}_i)=\mathbf{0}_{M/2}$

$$\begin{aligned}\iff\quad \mathbf{V}_{K-1}^T\mathbf{V}_{K-1}\prod_{i=K-2}^{0}(\mathbf{U}_i-\mathbf{V}_i) &= \mathbf{V}_{K-1}^T\mathbf{0}_{M/2}\\ \iff\quad \prod_{i=K-2}^{0}(\mathbf{U}_i-\mathbf{V}_i) &= \mathbf{0}_{M/2}\\ \iff\quad \mathbf{U}_{K-1}\prod_{i=K-2}^{0}(\mathbf{U}_i-\mathbf{V}_i) &= \mathbf{0}_{M/2}.\end{aligned}$$

This means that all symmetric filters have to be short as well, and we are left with an order-$(K-2)$ GenLOT. On the other hand, if all symmetric filters are short, so are all antisymmetric filters. □

In the next subsection, we shall show that it is possible to construct various VLLOT if some (but not all) of the symmetric (or antisymmetric) filters are short. Equivalently, it is possible to obtain

$$\mathbf{U}_{K-1}\prod_{i=K-2}^{0}(\mathbf{U}_i-\mathbf{V}_i)=\begin{bmatrix}\mathbf{X}_{N\times M/2}\\ \mathbf{0}_{(M/2-N)\times M/2}\end{bmatrix}$$

or

$$\mathbf{V}_{K-1}\prod_{i=K-2}^{0}(\mathbf{U}_i-\mathbf{V}_i)=\begin{bmatrix}\mathbf{X}_{N\times M/2}\\ \mathbf{0}_{(M/2-N)\times M/2}\end{bmatrix} \tag{21}$$

or even both.

C. Design Procedure

First, let us consider the case with $(M/2-N)$ short symmetric filters of length $M(K-1)$. Define the product $\mathbf{Tu}\triangleq\mathbf{U}_{K-1}\prod_{i=K-2}^{1}(\mathbf{U}_i-\mathbf{V}_i)$. It is possible to split $\mathbf{Tu}$'s row space into $\nu\triangleq\mathcal{S}\{\mathbf{tu}_1^T.,\mathbf{tu}_2^T.,\cdots,\mathbf{tu}_N^T.\}$ and the corresponding orthogonal complement $\nu^{\perp}$ [1]. Now, if we choose $(\mathbf{U}_0-\mathbf{V}_0)$ such that all of its columns lie in ν, then $\mathbf{U}_{K-1}\prod_{i=K-2}^{0}(\mathbf{U}_i-\mathbf{V}_i)=\mathbf{Tu}(\mathbf{U}_0-\mathbf{V}_0)$ will take the desired form

$$\begin{bmatrix}\mathbf{X}_{N\times M/2}\\ \mathbf{0}_{(M/2-N)\times M/2}\end{bmatrix}.$$

The following is an ordered outline of the designing steps:

- Choose arbitrary $M/2\times M/2$ orthogonal matrices $\mathbf{U}_{K-1}$, $\mathbf{B}$, and $\mathbf{U}_i$, $\mathbf{V}_i$, $i=1,2,\cdots,K-2$.
- Obtain the product $\mathbf{Tu}=\mathbf{U}_{K-1}\prod_{i=K-2}^{1}(\mathbf{U}_i-\mathbf{V}_i)$.
- Find an orthonormal basis for the first N rows of $\mathbf{Tu}$. Find an orthonormal basis for the corresponding orthogonal complement. From these orthonormal row vectors, form the unitary matrix $\mathbf{T}$.
- Obtain the first stage's building blocks by choosing

$$\mathbf{U}_0=\mathbf{T}\begin{bmatrix}\mathbf{Q}_1 & \mathbf{0}_{N\times(M/2-N)}\\ \mathbf{0}_{(M/2-N)\times N} & \mathbf{Q}_3\end{bmatrix}\mathbf{B}$$

and

$$\mathbf{V}_0=\mathbf{T}\begin{bmatrix}\mathbf{Q}_2 & \mathbf{0}_{N\times(M/2-N)}\\ \mathbf{0}_{(M/2-N)\times N} & \mathbf{Q}_3\end{bmatrix}\mathbf{B}$$

where $\mathbf{Q}_1$, $\mathbf{Q}_2$ are any $N\times N$ orthogonal matrices, and $\mathbf{Q}_3$ is any $(M/2-N)\times(M/2-N)$ orthogonal matrix.

With these particular choices of $\mathbf{U}_0$ and $\mathbf{V}_0$, the columns of the difference matrix $(\mathbf{U}_0-\mathbf{V}_0)$ can be easily verified to belong to the predefined subspace ν

$$\begin{aligned}\mathbf{U}_0-\mathbf{V}_0&=\mathbf{T}\begin{bmatrix}\mathbf{Q}_1 & \mathbf{0}\\ \mathbf{0} & \mathbf{Q}_3\end{bmatrix}\mathbf{B}-\mathbf{T}\begin{bmatrix}\mathbf{Q}_2 & \mathbf{0}\\ \mathbf{0} & \mathbf{Q}_3\end{bmatrix}\mathbf{B}\\ &=\mathbf{T}\left(\begin{bmatrix}\mathbf{Q}_1-\mathbf{Q}_2 & \mathbf{0}\\ \mathbf{0} & \mathbf{0}\end{bmatrix}\right)\mathbf{B}.\end{aligned}$$

The rotation angles of the arbitrary orthogonal matrices are the free parameters that can be tuned to optimize the VLLOT for any desired criterion. Note that we only have to put constraints on the first and last stage of the GenLOT's lattice structure to obtain the VLLOT of the same order. These two stages control the orthogonality between rows and columns of the building blocks to reduce the length of $((M/2)-N)$ filters by M. The constraints added to obtain VL reduce the total number of free parameters to optimized by

$$\binom{M/2}{2}-\left[2\binom{N}{2}+\binom{M/2-N}{2}\right].$$

The reduction is independent of the order K and can be significant for large M.

The same method can be applied to shorten any N antisymmetric filters, as long as N is less than $M/2$. If only N antisymmetric filters and N symmetric filters are desired to be long, we have to ensure that the matrix $\mathbf{Tv}\triangleq\mathbf{V}_{K-1}\prod_{i=K-2}^{1}(\mathbf{U}_i-\mathbf{V}_i)$ is appropriately chosen such

$$\mathbf{P}_K=\begin{bmatrix}\mathbf{X}_{N\times M/2} & \mathbf{X}_{N\times M/2} & \cdots & \mathbf{X}_{N\times M/2} & \mathbf{X}_{N\times M/2}\\ \mathbf{0}_{(M-N)\times M/2} & \mathbf{X}_{(M-N)\times M/2} & \cdots & \mathbf{X}_{(M-N)\times M/2} & \mathbf{0}_{(M-N)\times M/2}\end{bmatrix} \tag{19}$$

$$\mathbf{P}_K=\begin{bmatrix}\mathbf{U}_{K-1}\prod_{i=K-2}^{0}(\mathbf{U}_i-\mathbf{V}_i) & \mathbf{U}_{K-1}\prod_{i=K-2}^{1}(\mathbf{U}_i-\mathbf{V}_i)(\mathbf{U}_0+\mathbf{V}_0)\mathbf{J} & \cdots\\ \mathbf{V}_{K-1}\prod_{i=K-2}^{0}(\mathbf{U}_i-\mathbf{V}_i) & \mathbf{V}_{K-1}\prod_{i=K-2}^{1}(\mathbf{U}_i-\mathbf{V}_i)(\mathbf{U}_0+\mathbf{V}_0)\mathbf{J} & \cdots\end{bmatrix} \tag{20}$$

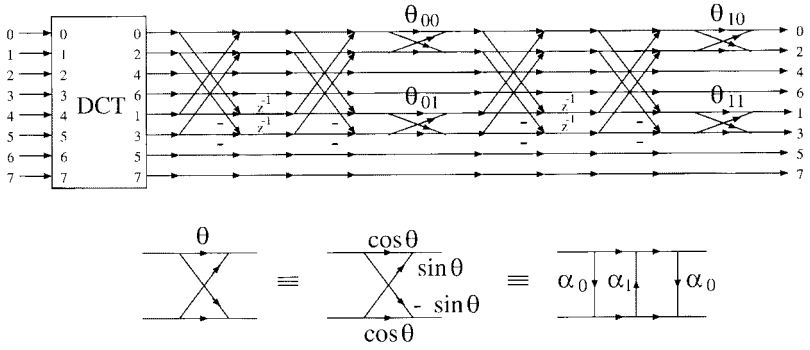

Fig. 7. The 4 × 24, 4 × 8 fast VLLOT.

TABLE II
COMPARISON OF TRANSFORM COMPLEXITY: NUMBER OF OPERATIONS NEEDED PER EIGHT TRANSFORM COEFFICIENTS

Transform	*No. of Multiplications*	*No. of Additions*	*Total No. of Ops.*
8 × 8 DCT	13	29	42
8 × 16 Type-II LOT	26	66	92
8 × 24 GenLOT	85	101	186
9/7 Wavelet, 1-level, standard	36	56	92
9/7 Wavelet, 3-level, standard	63	98	161
9/7 Wavelet, 1-level, lifting	24	32	56
9/7 Wavelet, 3-level, lifting	42	56	98
4 × 24 4 × 8 VLLOT	25	57	82

that its row space can be split into the same two orthogonal subspaces ν and $\nu^{\perp}$. We propose the following solution:

- Choose

$$\mathbf{V}_{K-1} = \begin{bmatrix} \mathbf{Q}_4 & \mathbf{0}_{N\times(M/2-N)} \\ \mathbf{0}_{(M/2-N)\times N} & \mathbf{Q}_5 \end{bmatrix} \mathbf{U}_{K-1}$$

where $\mathbf{Q}_4$, $\mathbf{Q}_5$ are, respectively, arbitrary $N \times N$ and $(M/2-N)\times(M/2-N)$ orthogonal matrices.

With this particular choice of $\mathbf{V}_{K-1}$, both of the VL properties in (21) can be satisfied simultaneously:

$$\begin{aligned} \mathbf{V}_{K-1} &\prod_{i=K-2}^{0} (\mathbf{U}_i - \mathbf{V}_i) \\ &= \begin{bmatrix} \mathbf{Q}_4 & \mathbf{0}_{N\times(M/2-N)} \\ \mathbf{0}_{(M/2-N)\times N} & \mathbf{Q}_5 \end{bmatrix} \\ &\quad \cdot \mathbf{U}_{K-1} \prod_{i=K-2}^{0} (\mathbf{U}_i - \mathbf{V}_i) \\ &= \begin{bmatrix} \mathbf{Q}_4 & \mathbf{0}_{N\times(M/2-N)} \\ \mathbf{0}_{(M/2-N)\times N} & \mathbf{Q}_5 \end{bmatrix} \\ &\quad \cdot \begin{bmatrix} \mathbf{X}_{N\times M/2} \\ \mathbf{0}_{(M/2-N)\times M/2} \end{bmatrix} \\ &= \begin{bmatrix} \mathbf{Q}_4\mathbf{X}_{N\times M/2} \\ \mathbf{0}_{(M/2-N)\times M/2} \end{bmatrix}. \end{aligned}$$

In this case, $\mathbf{V}_{K-1}$ contains $\left[\binom{N}{2} + \binom{M/2-N}{2}\right]$ degrees of freedom instead of $\binom{M/2}{2}$. Again, the reduction in the amount of free rotation angles is significant for large M.

This design method using orthogonal complement subspaces keys on the relationship between the GenLOT's building blocks $\mathbf{U}_i$ and $\mathbf{V}_i$ to obtain the coefficient matrix $\mathbf{P}$ directly. Hence, it can be classified as a time-domain design method. The resulting system is guaranteed to have LP as well as PR. Furthermore, the filters can have different lengths, yet all centers of symmetry are aligned. The FB can still be represented by a lattice structure. However, the VL property is not robust under the quantization of lattice coefficients.

V. FAST IMPLEMENTATION, OPTIMIZATION, AND DESIGN EXAMPLES

A. VLLOT Fast Implementation

This section is devoted to the design of a high-performance, yet low-complexity, VLLOT for image coding and processing applications.

To minimize the transform's complexity, we have to choose a small number of long filters, and set the initial stage $\mathbf{E}_0$ to be the DCT (which possesses numerous fast implementations). In the orthogonal case, it is easy to verify that setting the number of long filters to be two only yields trivial solutions since the matrices $\hat{\mathbf{U}}_i$ and $\hat{\mathbf{V}}_i$ degenerate to singleton 1 or -1, and there are not any free parameters for transform optimization. This is consistent with the well-known fact that the only two-channel linear-phase orthogonal filter bank is the Haar, $1/\sqrt{2}[1 \;\; 1; \; 1 \;\; -1]$. Hence, we have to increase the number of long filters to four. Their length is chosen to be 24-taps so that there is an overlap of eight pixels on either side, and traditional symmetric extension can be applied [8]. The short filters are still eight-tap. With this particular choice, there are four free rotation angles, and the resulting unnormalized lattice is illustrated in Fig. 7. Note that the four filters covering high-frequency spectrum of this fast VLLOT come straight from the DCT.

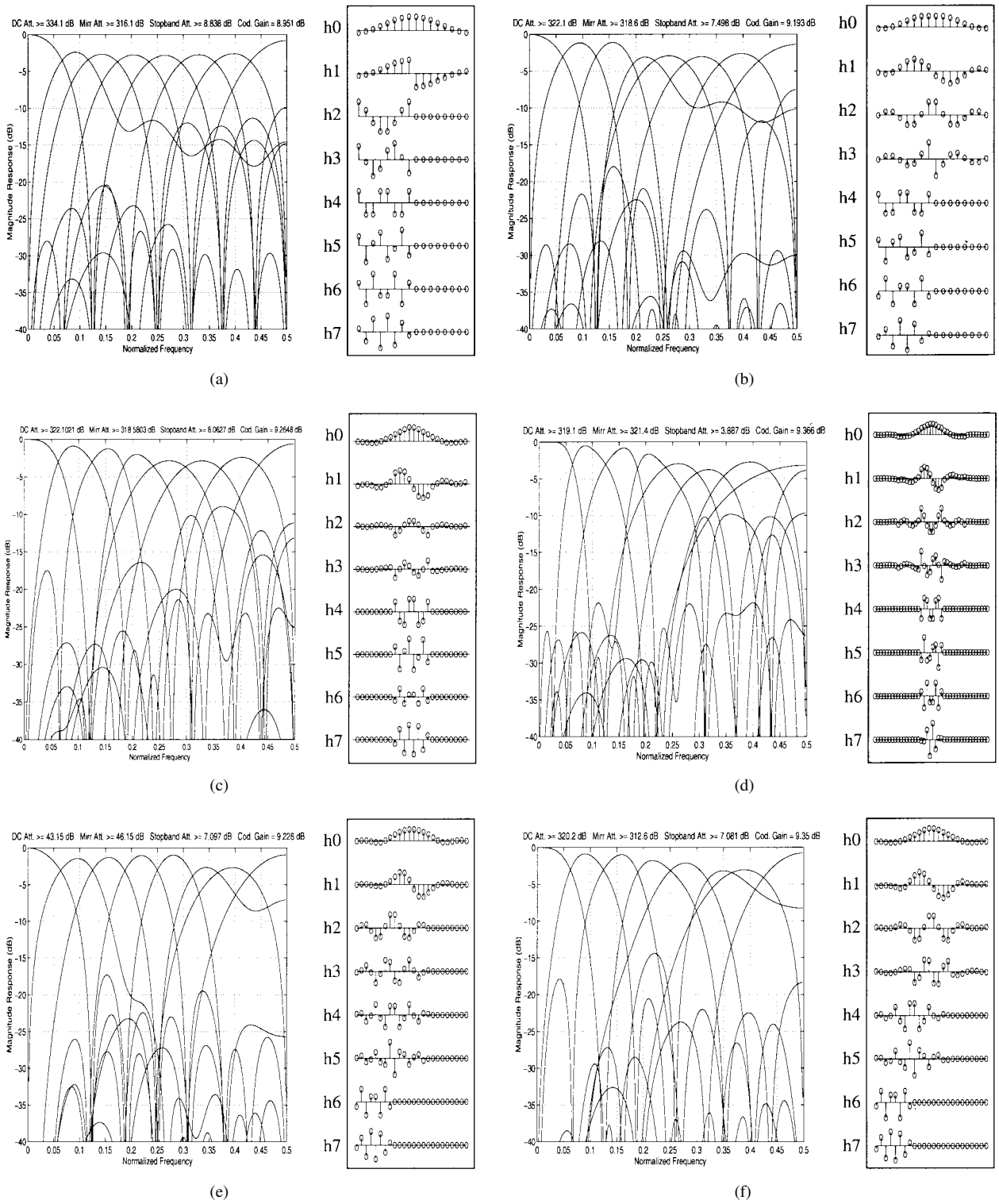

Fig. 8. Frequency and impulse responses of various transforms designed by direct lattice factorization method. (a) Two 16-tap and six eight-tap filters. (b) Four 16-tap and four eight-tap filters. (c) Four 24-tap and four eight-tap filters. (d) Four 40-tap and four eight-tap filters. (e) Four 24-tap, four 16-tap, and two eight-tap filters. (f) Four 24-tap, two 16-tap, and two eight-tap filters.

Since a plane rotation can be performed by three shears, i.e.,

$$\begin{bmatrix} \cos\theta_i & \sin\theta_i \\ -\sin\theta_i & \cos\theta_i \end{bmatrix} = \begin{bmatrix} 1 & 0 \\ \dfrac{\cos\theta_i - 1}{\sin\theta_i} & 1 \end{bmatrix} \begin{bmatrix} 1 & \sin\theta_i \\ 0 & 1 \end{bmatrix} \cdot \begin{bmatrix} 1 & 0 \\ \dfrac{\cos\theta_i - 1}{\sin\theta_i} & 1 \end{bmatrix}$$

where it takes three multiplications and three additions to implement each rotation. The multipliers are $\alpha_{i0} = (\cos\theta_i - 1)/\sin\theta_i$ and $\alpha_{i1} = \sin\theta_i$ (unless $\theta_i = k\pi$, $k \in \mathcal{Z}$; then, we only need two additions). The 1-D DCT requires 13 additions and 29 multiplications per eight transform coefficients. Therefore, the total number of operations needed to implement the

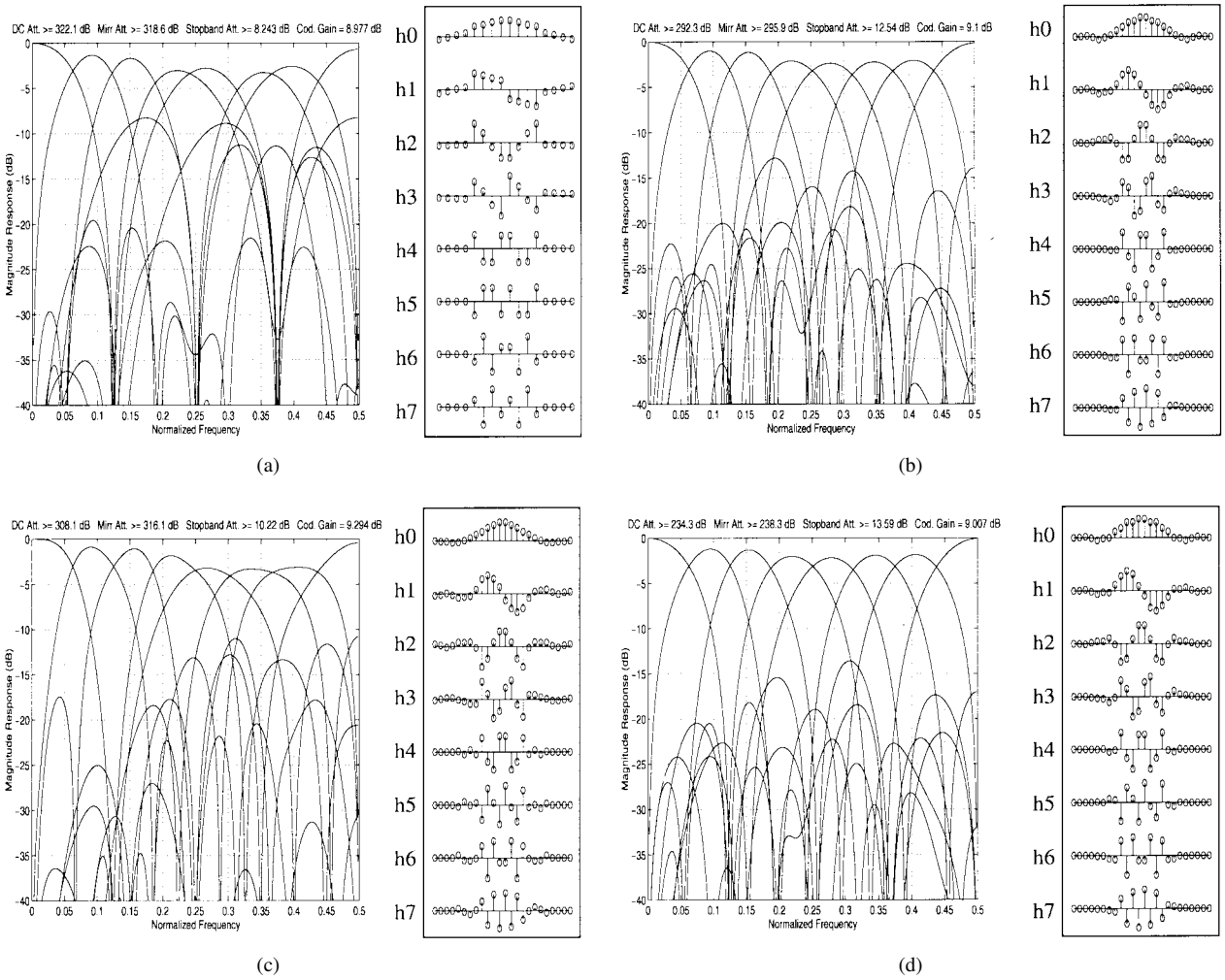

Fig. 9. Frequency and impulse responses of various transforms designed by the orthogonal complement subspace method. (a) Four 16-tap and four eight-tap filters. (b) Four 24-tap and four 16-tap filters, optimized for a balanced cost function. (c) Four 24-tap and four 16-tap filters, optimized primarily for coding gain. (d) Four 24-tap and four 16-tap filters, optimized primarily for stopband attenuation.

TABLE III
COMPARISON OF TRANSFORM PERFORMANCE

Transform	*Coding Gain (dB)*	*DC Att. (-dB)*	*Stopband Att. (-dB)*	*Mir. Att. (-dB)*
8×8 DCT	8.83	310.62	9.96	322.10
8×16 LOT	9.22	312.56	19.38	317.24
8×24 GenLOT	9.35	184.06	23.20	187.19
Fast VLLOT	9.26	322.10	8.06	318.58

fast 1-D VLLOT structure in Fig. 7 is 82: 25 additions and 57 multiplications.

A comparison of complexity between various popular transforms in 1-D is provided in Table II. The fast VLLOT's complexity is about twice that of the DCT (which is expected since the total filter lengths in the FB is doubled). It is slightly faster than the type-II fast LOT [6] and is much faster than the GenLOT of the same order (all filters are 24-tap). The 8×24 GenLOT has the highest complexity, even though its first stage has been set to be the DCT [4], [10]. Besides the first stage, the full 8×24 GenLOT employs four 4×4 orthogonal matrices; each in turn requires six plane rotations. The VLLOT in Fig. 7 is definitely faster than the 9/7-tap biorthogonal wavelet in both standard polyphase [2] or lifting implementation [11]. Keep in mind that the numbers of operations associated with the 9/7-tap pair in Table II come from only one level of decomposition. A deep dyadic decomposition needs roughly twice the tabulated 1-level amounts. Moreover, the wavelet transform requires a larger percentage of multiplication, which is typically slower than the addition in practical implementation.

B. Optimization Procedure

Any realization of the lattice coefficient set $\{\theta_i\}$ in the previous sections results in an LPPU system. However, for the VLLOT to have high practical value, several other properties are also needed. High-performance VLLOT can be obtained using unconstrained nonlinear optimization, where the lattice

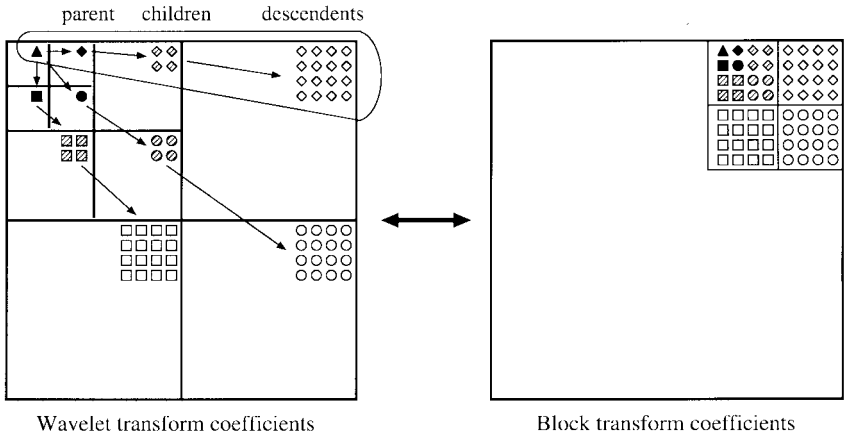

Fig. 10. Wavelet and block transform analogy.

coefficients are the free parameters. Since we are interested mainly in image coding applications, the cost function used in this paper is a weighted linear combination of coding gain, DC leakage, attenuation around mirror frequencies, and stopband attenuation—all of which are well-known desirable properties in yielding the best reconstructed image quality [2], [12]:

$$C_{\text{overall}} = \alpha_1 C_{\text{coding gain}} + \alpha_2 C_{\text{DC}} + \alpha_3 C_{\text{mirror}} + \alpha_4 C_{\text{stopband}}. \tag{22}$$

Among these criteria, higher coding gain correlates most consistently with higher objective performance (PSNR). Transforms with higher coding gain compact more energy into a fewer number of coefficients, and the more significant bits of those coefficients always get transmitted first in the progressive transmission framework employed in the later section. All design examples in this paper are obtained with a version of the paraunitary coding gain formula [6]

$$C_{\text{coding gain}} = 10 \log_{10} \frac{\sigma_x^2}{\left(\prod_{k=0}^{M-1} \sigma_{x_i}^2 \right)^{1/M}} \tag{23}$$

where σ_x^2 is the variance of the input signal, and $\sigma_{x_i}^2$ is the variance of the ith subband. The signal $x[n]$ is the commonly used AR(1) process with intersample autocorrelation coefficient $\rho = 0.95$.

Low DC leakage and high attenuation near the mirror frequencies are not as essential to the objective performance as coding gain. However, they do improve the visual quality of the reconstructed image significantly by alleviating annoying blocking and checkerboard artifacts. Finally, the stopband attenuation cost helps in improving the signal decorrelation, decreasing the amount of aliasing, and enhancing the smoothness of the filters. These cost functions are defined as follows:

$$C_{\text{DC}} = \sum_{i=1}^{M-1} \sum_{n=0}^{L-1} h_i[n] \tag{24}$$

$$C_{\text{mirror}} = \sum_{i=0}^{M-1} \left| H_i\left(e^{j\omega_m}\right) \right|^2, \qquad \omega_m = \frac{2\pi m}{M}$$
$$1 \le m \le \frac{M}{2} \tag{25}$$

TABLE IV
OBJECTIVE CODING RESULT COMPARISON (PSNR IN dB)

	Barbara			
Comp. Ratio	9/7-tap Wavelet	8×8 DCT	8×16 LOT	4×24 4×8 VLLOT
1:8	36.41	36.31	37.43	36.78
1:16	31.40	31.11	32.70	31.96
1:32	27.58	27.28	28.80	28.18
1:64	24.86	24.58	25.70	25.39
1:100	23.76	23.42	24.34	24.25
	Boat			
Comp. Ratio	9/7-tap Wavelet	8×8 DCT	8×16 LOT	4×24 4×8 VLLOT
1:8	39.11	38.93	39.26	39.17
1:16	34.46	34.20	34.61	34.52
1:32	30.97	30.43	30.93	30.89
1:64	28.16	27.52	28.07	28.09
1:100	26.66	25.88	26.40	26.42
	Lena			
Comp. Ratio	9/7-tap Wavelet	8×8 DCT	8×16 LOT	4×24 4×8 VLLOT
1:8	40.41	39.91	40.09	40.10
1:16	37.21	36.38	36.75	36.76
1:32	34.12	32.90	33.57	33.56
1:64	31.10	29.67	30.48	30.54
1:100	29.35	27.80	28.61	28.81

$$C_{\text{stopband}} = \sum_{i=0}^{M-1} \int_{\omega \in \Omega_{\text{stopband}}} \left| H_i\left(e^{j\omega}\right) \right|^2 d\omega. \tag{26}$$

The set of $\{\alpha_i\}$ in (22) controls the tradeoff between various FB characteristics. We found that the set $\{1, 1, 0.1, 0.1\}$ typically works well in optimizing FB's for image coding. To initialize the lattice, we set all lattice coefficients to π.

In an alternative (and faster) design procedure, the filters are first obtained from the iterative method based on time-domain constraints [13]. Then, the lattice coefficients can then be calculated from the resulting FB coefficients.

C. Design Examples

We present in this section several VLLOT examples using the design approaches previously discussed in Sections III and IV and the optimization methods described in Section V-B.

Fig. 11. Reconstructed boat images at 1 : 32 compression ratio. Top left: 8 × 8 DCT, 30.43 dB. Top right: 8 × 16 type-II fast LOT, 30.93 dB. Bottom left: 9/7-tap biorthogonal wavelet, 30.97 dB. Bottom right: 4 × 24 4 × 8 fast VLLOT, 30.89 dB.

The magnitude and the impulse responses of the new VLLOT's obtained directly from the VL lattice structure are depicted in Fig. 8. The fast VLLOT discussed in Section V-A is shown in Fig. 8(c). The new VLLOT's designed by the orthogonal complement subspace method are shown in Fig. 9.

The objective performance measures of several VLLOT's and other block transforms in previous works are tabulated and compared in Table III. Given the same order K, the VLLOT cannot match the GenLOT in terms of objective characteristics (coding gain and stopband attenuation for example) because it belongs to a subclass of GenLOT. However, the VLLOT's variable-length basis functions make it significantly faster than the GenLOT of the same order (see Table II). The coding gain of the fast VLLOT is also slightly higher than that of the quasioptimal LOT [6]. Note that since the application we have in mind is image compression, all presented FB examples have highband filters chosen to be short. The design methods do us to shorten other filters if we want to.

VI. Application in Image Coding

The coding performance of the new VLLOT is evaluated through an image coding comparison. To be fair, the same transform-based progressive image coder SPIHT [14] is used in all cases. The difference lies at the transform stage, where the five transforms in comparison are the following:

- the DCT, eight filters, all 8-tap, shown in Fig. 3(a);
- the type-II fast LOT, eight filters, all 16-tap, shown in Fig. 3(b);
- the fast VLLOT, four 24-tap and four 8-tap filters, shown in Fig. 8(c);
- the popular 9/7-tap biorthogonal wavelet in [15].

In the block-transform case, we have to modify the zerotree structure. Each block of lapped transform coefficients represents a spatial locality similarly to a tree of wavelet coefficients. A wavelet tree in an L-level decomposition is analogous to a 2^L-channel transform's coefficient block, as illustrated in Fig. 10. The difference lies at the bases that generate these coefficients. Let $\mathcal{O}(i, j)$ be the set of coordinates of all offspring of the node (i, j) in an M-channel uniform-band block transform $(0 \leq i, j \leq M-1)$; then, $\mathcal{O}(i, j)$ can be represented as

$$\mathcal{O}(i, j) = \{(2i, 2j), (2i, 2j+1), (2i+1, 2j) \\ (2i+1, 2j+1)\}.$$

All (0, 0) coefficients from all transform blocks form the DC band, which is similar to the wavelet transform's reference

Fig. 12. Reconstructed Lena images at 1 : 32 compression ratio. Top left: 8 × 8 DCT, 32.90 dB. Top right: 8 × 16 type-II fast LOT, 33.57 dB. Bottom left: 9/7-tap biorthogonal wavelet, 34.11 dB. Bottom right: 4 × 24 4 × 8 fast VLLOT, 33.56 dB.

signal; each of these nodes has only three offspring: (0, 1), (1, 0), and (1, 1). This is a straightforward generalization of the structure first proposed in [16]. The only requirement here is that the number of channels M has to be a power of two. With this modified tree definition, any zerotree coder can be used to encode the transform coefficients.

To decorrelate the DC band even more, several levels of wavelet decomposition can be applied on the DC band, depending on the input image size. This step increases the coding efficiency of the DC coefficients thanks to a deeper coefficient trees. Besides, it offers a fair comparison between the transforms since the SPIHT coder uses up to six levels of wavelet decomposition on 512 × 512 images, whereas the 8-channel block transforms only provide an equivalence of 3-level decomposition. For more details on the embedded coding algorithms, see [14], [17], and [18].

The three images chosen for the coding experiments are Barbara, Boat, and Lena. All of them are standard, well-known 512 × 512 8-bit gray-scale test images. The objective distortion measure is the popular peak signal-to-noise ratio (PSNR)

$$\text{PSNR} = 10 \log_{10} \left(\frac{255}{\text{MSE}} \right) \text{dB}$$

where MSE denotes the mean squared error between the original and the reconstructed image. The PSNR's from using various transforms at various bit rates are tabulated in Table IV. All computed PSNR quotes are obtained from real compressed bit streams with all overheads included.

The coding results from Table IV and Figs. 11–13 demonstrate that the novel VLLOT provides an interesting tradeoff between transform complexity and coding performance. Objectively, the VLLOT is clearly superior to the DCT in all three test images at all bit rates. It is also very comparable with the quasioptimal type-II fast LOT. In the complex Barbara image, where there is a large amount of texture, the VLLOT's poor frequency resolution in the higher frequency spectrum (due to the four filters from the DCT) translates to an inferior performance compared with the LOT. However, in smoother images such as Boat and Lena, the VLLOT's and the LOT's performance is very similar; the VLLOT starts to outperform the LOT at lower bit rates (a wavelet characteristic). Compared the 9/7-tap biorthogonal wavelet, the VLLOT offers a lower performance in Lena. Nevertheless, in the Boat image, where there is a fair amount of edges and texture, the two transforms yield almost identical objective results. In the more complex Barbara image, the VLLOT can outperform the wavelet trans-

Fig. 13. Enlarged 256 × 256 portions of reconstructed Lena images at 1 : 32 compression ratio. Top left: 8 × 8 DCT. Top right: 8 × 16 type-II fast LOT. Bottom left: 9/7-tap biorthogonal wavelet. Bottom right: 4 × 24 4 × 8 fast VLLOT.

form by more than 0.5 dB over a wide range of bit rates (0.125–0.25 b/pixel).

Subjectively, the VLLOT's reconstructed images generally possess smooth, visually pleasant, wavelet-like characteristics, as illustrated in Figs. 11–13. Blocking artifacts are alleviated significantly, whereas ringing artifacts are effectively contained. A closer look in Fig. 13 (where enlarged 256 × 256 image portions are shown so that artifacts can be more easily seen) reveals that the VLLOT yields no annoying blocking and excessive ringing artifacts. In fact, the VLLOT is even slightly better than the LOT in blocking removal. The edges around the lips, the eyes, and the shoulder are reconstructed faithfully.

VII. Conclusions

In this paper, the theory, design, and lattice structure of LPPUFB with filters of different lengths have been presented and analyzed in detail. The proposed lattice structure is robust under coefficient quantization: It retains all attractive properties of the FB (LP, PU, and variable-length), and it has fast and efficient implementation. The lattice also spans the complete class of all permissible solutions: The number of long filters must be even; half of the long filters are symmetric, and the other half are antisymmetric and so are the short filters. Another design method that keys on the relationship between the GenLOT lattice coefficients to obtain variable-length filters is also discussed.

The new FB can be interpreted as a class of lapped orthogonal transforms with basis functions of variable lengths that we labeled as VLLOT. The VLLOT's initial stage can be chosen to be the DCT so that existing fast software and hardware implementation can be employed. This new lapped transform finds application in transform-based image compression since it relies on its long basis functions to reconstruct smooth signal components while it uses short basis functions to represent edges and textures. Experimental results show great promise of the proposed transform: Blocking artifacts in DCT are alleviated while ringing artifacts in GenLOT are contained. Moreover, both of these can be achieved at a very reasonable level of complexity. The VLLOT is certainly a step toward a better understanding of how to design filter banks that are most suited to the human visual system.

Compared with the popular wavelet transform, the VLLOT's block-based nature allows fast, simple, and efficient one-pass block coding if we so desire. Besides the lower

computational complexity, computational parallelism, region-of-interest coding/decoding efficiency, and the capability of processing large images under limited resource constraints are several other advantages that VLLOT offers over the wavelet transform.

REFERENCES

[1] P. P. Vaidyanathan, *Multirate Systems and Filter Banks.* Englewood Cliffs, NJ: Prentice-Hall, 1993.

[2] G. Strang and T. Q. Nguyen, *Wavelets and Filter Banks.* Wellesley, MA: Cambridge, 1996.

[3] A. Soman, P. P. Vaidyanathan, and T. Q. Nguyen, "Linear phase paraunitary filter banks: Theory, factorizations, and applications," *IEEE Trans. Signal Processing,* vol. 41, pp. 3480–3496, Dec. 1993.

[4] R. de Queiroz, T. Q. Nguyen, and K. Rao, "The GenLOT: Generalized linear-phase lapped orthogonal transform," *IEEE Trans. Signal Processing,* vol. 40, pp. 497–507, Mar. 1996.

[5] W. B. Pennebaker and J. L. Mitchell, *JPEG: Still Image Compression Standard.* New York: Van Nostrand Reinhold, 1993.

[6] H. S. Malvar, *Signal Processing with Lapped Transforms.* Norwell, MA: Artech House, 1992.

[7] T. D. Tran and T. Q. Nguyen, "On M-channel linear-phase FIR filter banks and application in image compression," *IEEE Trans. Signal Processing,* vol. 45, pp. 2175–2187, Sept. 1997.

[8] R. de Queiroz and K. R. Rao, "On reconstruction methods for processing finite-length signals with paraunitary filter banks," *IEEE Trans. Signal Processing,* vol. 43, pp. 2407–2410, Oct. 1995.

[9] R. de Queiroz, "On lapped transforms," Ph.D. dissertation, Univ. Texas, Arlington, Dec. 1994.

[10] S. Trautmann and T. Q. Nguyen, "GenLOT—Design and application for transform-based image coding," in *Proc. 29th Asilomar Conf. SSC,* Pacific Grove, CA, Nov. 1995.

[11] I. Daubechies and W. Sweldens, "Factoring wavelet transforms into lifting steps," *J. Fourier Anal. Appl.,* vol. 4, pp. 247–269, 1998.

[12] T. A. Ramstad, S. O. Aase, and J. H. Husoy, *Subband Compression of Images: Principles and Examples.* New York: Elsevier, 1995.

[13] M. Ikehara and T. Q. Nguyen, "Time-domain design of perfect reconstruction filter banks with linear phase," in *Proc. IEEE Int. Conf. Acoust., Speech, Signal Process.,* Munich, Germany, May 1997.

[14] A. Said and W. A. Pearlman, "A new fast and efficient image codec based on set partitioning in hierarchical trees," *IEEE Trans. Circuits Syst. Video Technol.,* vol. 6, pp. 243–250, June 1996.

[15] M. Antonini, M. Barlaud, P. Mathieu, and I. Daubechies, "Image coding using wavelet transform," *IEEE Trans. Image Processing,* vol. 1, pp. 205–220, Apr. 1992.

[16] Z. Xiong, O. Guleryuz, and M. T. Orchard, "A DCT-based embedded image coder," *IEEE Signal Processing Lett.,* vol. 3, pp. 289–290, Nov. 1996.

[17] T. D. Tran and T. Q. Nguyen, "A progressive transmission image coder using linear phase filter banks as block transforms," *IEEE Trans. Image Processing,* to be published.

[18] ——, "A lapped transform embedded image coder," in *Proc. IEEE Int. Symp. Circuits Syst.,* Monterey, CA, May 1998.

[19] ——, "Generalized lapped orthogonal transform with unequal-length basis functions," in *Proc. IEEE Int. Symp. Circuits Syst.,* Hong Kong, June 1997.

[20] M. Ikehara, T. D. Tran, and T. Q. Nguyen, "Linear phase paraunitary filter banks with unequal-length filters," in *Proc. IEEE Int. Conf. Image Process.,* Santa Barbara, CA, Oct. 1997.

[21] C. W. Kok, M. Ikehara, and T. Q. Nguyen, "Structures and factorizations of linear-phase paraunitary filter banks," in *Proc. IEEE Int. Symp. Circuits Syst.,* June 1997, pp. 365–368.

[22] L. Chen, K. P. Chan, T. Q. Nguyen, and Y. Zheng, "A new synthesis procedure for linear-phase paraunitary digital filter banks," in *Proc. IEEE Int. Symp. Circuits Syst.,* June 1997, pp. 2377–2380.

[23] F. R. Gantmacher, *The Theory of Matrices.* New York: Chelsea, 1977.

Trac D. Tran (M'98) received the B.S. and M.S. degrees from the Massachusetts Institute of Technology, Cambridge, in 1994 and the Ph.D. degree from the University of Wisconsin, Madison, in 1998, all in electrical engineering.

He joined the faculty of The Johns Hopkins University, Baltimore, MD, in July 1998 as an Assistant Professor with the Department of Electrical and Computer Engineering. His research interests are in the field of digital signal processing, particularly in multirate systems, filter banks, wavelets, and their applications in signal representation, compression, and processing.

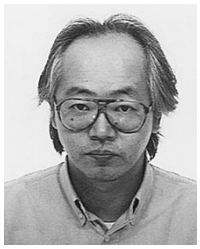

Masaaki Ikehara (M'92) received the B.E., M.E., and Dr.Eng. degrees in electrical engineering in 1984, 1986, and 1989, respectively, from Keio University, Yokohama, Japan.

From 1989 to 1992, he was an Assistant Professor in the Department of Electrical Engineering and Computer Science, Nagasaki University, Nagasaki, Japan. In 1992, he joined the Faculty of Engineering, Keio University. From 1996 to 1998, he was a Visiting Researcher at the University of Wisconsin, Madison, and Boston University, Boston, MA. He is currently an Associate Professor of Electronics and Electrical Engineering at Keio University. His research interests are in the areas of multirate signal processing, wavelet image coding, and filter design problems.

Truong Q. Nguyen (SM'95) received the B.S., M.S., and Ph.D. degrees in electrical engineering from the California Institute of Technology, Pasadena, in 1985, 1986, and 1989, respectively.

He was with Lincoln Laboratory, Massachusetts Institute of Technology (MIT), Lexington, from June 1989 to July 1994 as a Member of Technical Staff. From 1993 to 1994, he was a Visiting Lecturer at MIT and an Adjunct Professor at Northeastern University, Boston, MA. He was with the Electrical and Computer Engineering Department, University of Wisconsin, Madison, from August 1994 to April 1998. Since July 1996, he has been with the Electrical and Computer Engineering Department, Boston University, Boston, MA. His research interests are in digital and image signal processing, image and video compression, multirate systems, wavelets and applications, biomedical signal processing, filter design, and A/D converters.

Prof. Nguyen was the recipient of a fellowship from Aerojet Dynamics for advanced studies. He received the IEEE TRANSACTIONS IN SIGNAL PROCESSING Paper Award (Image and Multidimensional Processing area) for the paper he coauthored with Prof. P. P. Vaidyanathan on linear-phase perfect-reconstruction filter banks in 1992. He received the NSF Career Award in 1995 and is the coauthor (with Prof. G. Strang) of the textbook *Wavelets and Filter Banks* (Cambridge, MA: Wellesley, 1996). He was an Associate Editor for the IEEE TRANSACTIONS ON SIGNAL PROCESSING and for the IEEE TRANSACTIONS ON CIRCUITS AND SYSTEMS II and has also served in the DSP Technical Committee for the IEEE Circuits and Systems Society. He is a member of Tau Beta Pi, Eta Kappa Nu, and Sigma Xi.